Current Status of Novel Gratings for Next Generation Astronomical Instruments IV

N. Ebizuka[1], T. Okamoto[1], T. Hosobata[1], Y. Yamagata[1], M. Sasaki[2], M. Uomoto[3], T. Shimatsu[3], S. Sato[4], N. Hashimoto[4], O. Kirino[5], I. Tanaka[6], T. Hattori[6], S. Ozaki[6], W. Aoki[6]

[1] RIKEN, [2] Toyota Technological Institute, [3] Tohoku University, [4] CITIZN Holdings Co. Ltd., [5] Crystal Optics Co. Ltd., [6] National Astronomical Observatory, Japan

Birefringence volume phase holographic (B-VPH) grating

$$\eta_S = \sin^2\left\{\frac{\pi\left(n_{S\max}-n_{S\min}\right)t}{\Lambda\left(n_{S\max}+n_{S\min}\right)\sin 2\theta_S}\right\} \qquad \eta_P = \sin^2\left\{\frac{\pi\left(n_{P\max}-n_{P\min}\right)t\cos 2\theta_P}{\Lambda\left(n_{P\max}+n_{P\min}\right)\sin 2\theta_P}\right\}$$

$$\frac{\left(n_{S\max}-n_{S\min}\right)}{\left(n_{S\max}+n_{S\min}\right)*2\sin\theta_S\cos\theta_S} = \frac{\left(n_{P\max}-n_{P\min}\right)\cos 2\theta_P}{\left(n_{P\max}+n_{P\min}\right)*2\sin\theta_P\cos\theta_P}$$

$$\frac{\left(n_{S\max}-n_{S\min}\right)}{\left(n_{S\max}+n_{S\min}\right)\sin 2\theta_S} = \frac{\left(n_{P\max}-n_{P\min}\right)\cos 2\theta_P}{\left(n_{P\max}+n_{P\min}\right)\sin 2\theta_P} \qquad \frac{\left(n_{S\max}-n_{S\min}\right)}{\cos\theta_S} = \frac{\left(n_{P\max}-n_{P\min}\right)\cos 2\theta_P}{\cos\theta_P}$$

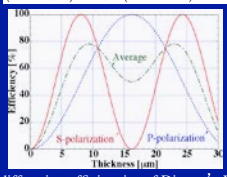

Polarized diffraction efficiencies of Dicson's VPH grating (Polarizer) calculated by Kogelnik method. Λ= 0.646, n_L= 1.46, n_H=1.54, θ_B=48.5°.

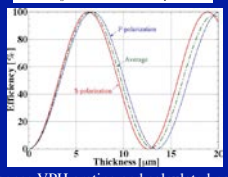

Birefringence VPH grating and calculated polarized diffraction efficiencies versus grating thick-ness *t*. Λ= 0.646 μm, n_L=1.46, n_s= 1.544, n_p = 1.60, θ_B=45°.

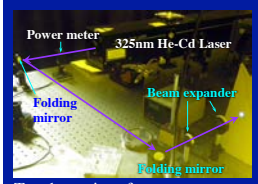

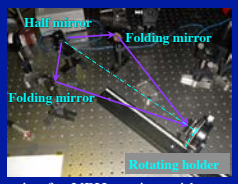

Two beam interference exposure optics for VPH grating with UV curable LC.

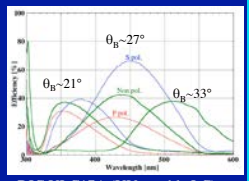

DIC ULC17A (UV curable LC) +Merck MJ041609 (normal LC), Λ~ 0.5 μm, t=10 μm.

Echelle grism for MOIRCS

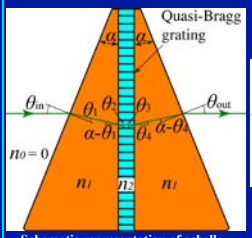

Schematic representation of echelle grism for MOIRCS

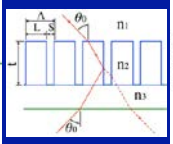

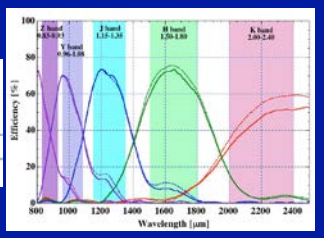

L&S=4.6:0.5 [μm], θ_0=28.4°, n_1=1.33, n_2=1.6, n_3=1.6, t = 16 μm

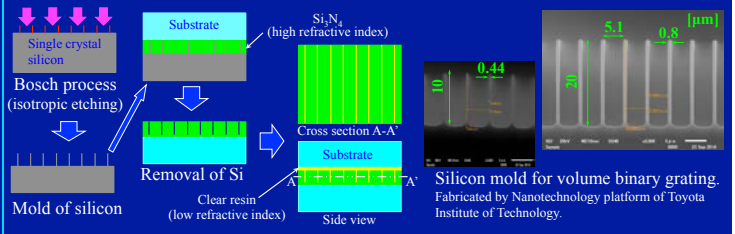

Silicon mold for volume binary grating. Fabricated by Nanotechnology platform of Toyota Institute of Technology.

Fabrication process of the volume binary grating

Limitation of surface relief (SR) grating

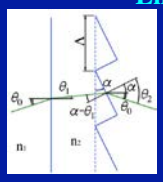

$$\sin\theta_0 = n\sin\theta_1$$
$$n\sin(\alpha-\theta_1) = \sin\theta_2$$
$$\theta_2 = \alpha+\theta_0$$
$$n\sin(\alpha-\theta_1) = \sin(\alpha+\theta_0)$$
$$n(\sin\alpha\cos\theta_1 - \sin\theta_1\cos\alpha) = \sin\alpha\cos\theta_0 + \sin\theta_0\cos\alpha$$
$$(n\cos\theta_1 - \cos\theta_0)\sin\alpha = (\sin\theta_0 + n\sin\theta_1)\cos\alpha$$
$$= 2\sin\theta_0\cos\alpha$$
$$\tan\alpha = 2\sin\theta_0 / (n\cos\theta_1 - \cos\theta_0)$$

n = 1.5, $\theta_0 \le 30°$ ($\theta_2 > 90°$)
n = 1.8, $\theta_0 \le 36°$
n = 2.3, $\theta_0 \le 45°$
n = 3.0, $\theta_0 \le 54°$
Diamond: n = 2.46@400nm

SR grating with saw tooth grooves is not feasible for the high-dispersion transmission grating.

Reflector facet transmission (RFT) grating

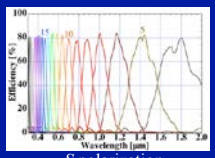

S polarization

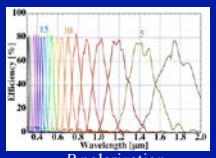

P polarization

Λ=5μm, θ_0=45°, n_1=1.0, n_2=1.54

RTF gratings for WFOS of TMT
Groove vertex angle : γ = 35~45°
Grating period : Λ= 2~5 μm

Hybrid grism for MOIRCS

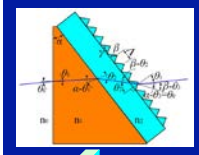

Prism material	: ZnSe (n_1= 2.4529@1.65 μm)
Plate	: S-FPM3 (n_2= 1.5240@1.65 μm)
Prism vertex angle	: α = 23.8°
Grating period	: Λ= 10.79μm (92.68 grooves/mm)
Incident angle	: θ_0= 5°
Groove blaze angle	: β = 64.8°
Groove vertex angle	: γ = 61.8°

Slit width: 0.3"
7th, R= 2,900@0.88 μm
6th, R= 2,790@1.02 μm
5th, R= 2,750@1.25 μm
4th, R= 2,800@1.65 μm
3rd, R= 2,770@2.20 μm

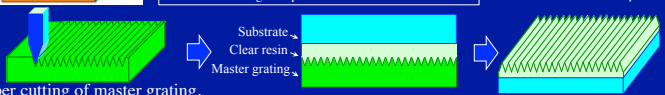

Shaper cutting of master grating.
Work: Ni-P alloy of non-electrolytic plating

Replication

Finish

Fabrication method of SR grating for RFT grating and MOIRCS hybrid grism

Ultra-high precision machine (Nagase-I, NPIC-M200).

Single-crystal diamond tool.

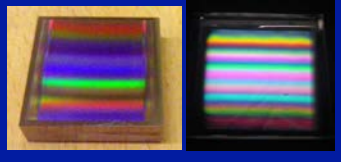

Mold for replication experiment (left), replica of mold (right). Work piece size: 50×50 [mm].

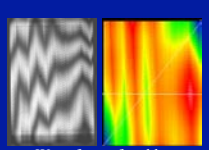

Wave front of mold.
PV:0.89λ, RMS: 0.13λ.

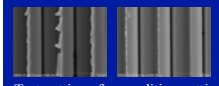

Test cuttings for condition setting.

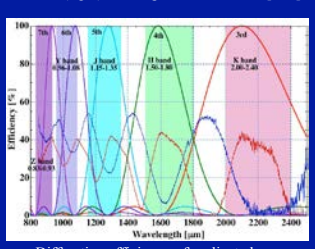

Diffraction efficiency of replicated transmission grating.

Quasi-Bragg immersion grating

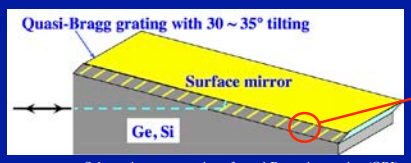

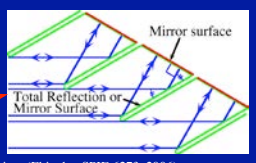

Schematic representation of quasi-Bragg immersion (QBI) grating. (Ebizuka, SPIE 6273, 2006)

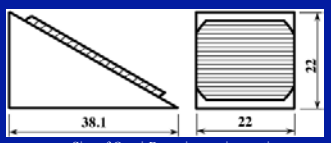

Size of Quasi-Bragg immersion grating

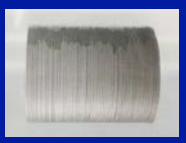

Block of mirror substrates stacked by fusion of gold.

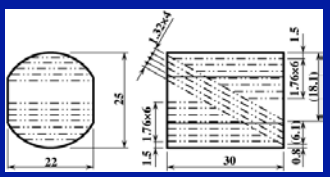

Cutting position of wire saw

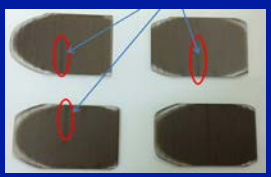

Quasi-Bragg grating with tilted mirror lattice.

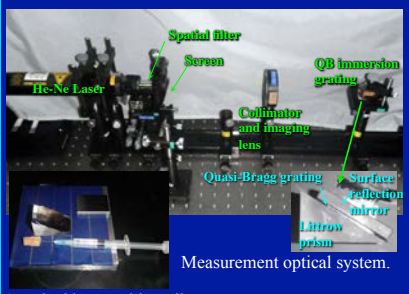

Measurement optical system.

Attached by matching oil

Diffraction pattern (about 1,000th order) of QB grating. Beam is split up and down.

The diffracted beam is concentrated (blazed). However diffraction orders cannot separate because a point source image is larger than the interval of the diffraction orders (about 2,000th orders).

Summary

	Optimal Order	Eff. [%] (λ-λ [μm])	Status of development
VPH grating →LC VPH grating	1st	~90 →~100 (0.32~2.4)	Installed in FOCAS, MOIRCS, Kools and WSGS2. (photopolymer)
Reflector facet transmission grating	2th~	~ 80 (0.32~2.4)	Evaluations of diffraction efficiency by numerical calculations of RCWA.
Hybrid grism	2rd~	~ 80 (0.32~2.4)	Performing diamond cutting of a master grating of Ni-P alloy for MOIRCS.
Volume binary grating	1st~	~ 80 (0.2~1000)	Performing test fabrications by using MEMS technique.
Quasi-Bragg immersion grating	5th~	~ 80 (0.2~1000)	Performed test fabrications of lamination by atoms fusion bonding and lamination of embossed substrates.